
2 GHz 대역 RF 대역통과 필터 응용을 위한 AlN 압전 박막을 이용한 FBAR 소자

윤기완* · 임문혁* · 채동규* · 김종현**

FBAR Device with Thin AlN Piezoelectric Film for 2 GHz RF Bandpass Filter Applications

Giwan Yoon* · Munhyuk Yim* · Dongkyu Chai* · Sanghee Kim** · Jongheon Kim**

This work was partially supported by Korea Research Foundation Grant (KRF-2002-003-D00229)

요 약

본 논문에서는 2GHz 대역 RF 대역통과 필터 응용을 위한 FBAR 소자에 대한 연구를 발표한다. 본 연구의 FBAR 소자는 크게 상부 및 하부 전극 사이에 압전체(AlN)가 삽입되어 있는 공진부와 SiO₂/W 이 여러층으로 적층되어 있는 음향반사층 두 부분으로 구성되어 있다. RF sputtering 방법으로 증착된 AlN 박막은 c축이 기판에 수직인 정도가 우수한 c축 우선 배향성을 갖는다. 이때 결정립(grain)은 길고 얇은 주상형(columnar)을 보인다. 뿐만아니라, 우수한 품질계수(4300)와 반사손실(37.19 dB)도 얻어졌다.

ABSTRACT

A film bulk acoustic resonator (FBAR) device for 2 GHz radio frequency (RF) bandpass filter application is presented. This FBAR device consists of an aluminum nitride (AlN) film sandwiched between top(Al) and bottom(Au) electrodes and an acoustic multilayer reflector of a silicon dioxide/tungsten (SiO₂/W). The AlN film deposited using a RF sputtering was observed to have small columnar grains with a strongly preferred orientation towards c axis. In addition to a high quality factor (4300), a large return loss of 37.19 dB was obtained.

Keyword

FBAR, AlN film, Multilayer Reflector, Return Loss, Quality Factor

1. Introduction

Recently, the explosion in wireless communications services has strongly demanded even higher performance in RF filter devices. In general, the commercial RF bandpass filters are based on ceramic and surface acoustic

wave(SAW) resonators[1] due to their superiorities in insertion loss and attenuation, respectively. Unfortunately, these RF filters can hardly be integrated with other devices and still remain as off-chip components, inevitably causing large parasitics. The FBAR technology seems very promising for

*한국정보통신대학교

**광운대학교

integrating a bandpass filter function into silicon because it can be compatibly integrated with other silicon devices, suggesting its strong potential for the realization of monolithic microwave integrated circuits(MMICs) in the future. From the silicon processing point of view, AlN film[2] seems to be more preferred to ZnO film[3] mainly because zinc(Zn) forms a deep-level trap and has a high vapor pressure.

In this article, we present the fabrication and analysis results of the FBAR with an AlN piezoelectric film and a six-layer reflector layer for 2 GHz RF bandpass filter application.

II. Experiments

A two-port FBAR was fabricated using a sputtering system. The reflector consists of SiO₂ and W layers. On a precleaned silicon substrate, SiO₂ and W films were alternately deposited to form a six-layer reflector layer. For bottom electrode formation, Au film was deposited on top of the multilayer reflector. Conventional photolithography was performed for electrodes patterning. Then, AlN film was deposited for piezoelectric layer formation, followed by the Al deposition for the top electrode. Each electrode thickness was controlled to be 1300Å using an electron beam evaporator. It is noted that both Al and Au films were deposited with silicon substrate rotated at 15 rpm. The schematic of the FBAR is illustrated in Fig. 1.

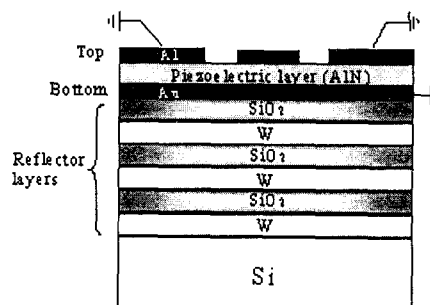


Fig. 1 Schematic cross-sectional view of FBAR device.

Table 1. Deposition conditions of AlN, W, SiO₂, Al and Au films.

Film	AlN	W	SiO ₂	Au,Al
Deposition System	RF magnetron sputter			ebeam
Pressure(mTorr)	5	7.1		
Power(W)	200	150	300	3000
Gas flow rate	Ar+N ₂		Ar	
Distance	6	7.6		40
Deposition Time(min)	260	100	30	30

The top surface has a normal air while the bottom surface has a six-layer reflector solidly mounted on silicon. The film deposition conditions are summarized in Table 1.

III. Results and Discussion

The FBAR structure is thought of as an acoustic transmission line that can be analyzed in a similar way to an electrical transmission line [4]. Across each material layer, the effective input impedance due to the standing wave can be given by the following transmission equation:

$$Z_i = Z_c \left[\frac{Z_L \cos \theta + j Z_c \sin \theta}{Z_c \cos \theta + j Z_L \sin \theta} \right] \quad (1)$$

where Z_i is the input impedance, Z_c the characteristic impedance, Z_L the load impedance of the section, and θ the total phase across the section. Since the thickness of one quarter-wavelength ($\lambda/4$) leads to $\theta = \pi/2$, the electrical input impedance (Z_i) will be:

$$Z_i = \frac{Z_c^2}{Z_L} \quad (2)$$

Based on equation (2), the input impedance ($Z_{i(1)}$) at piezoelectric film layer of Fig. 2 can be derived as equation (3). The normalized input impedance (z) can be expressed by equation (4). The reflection coefficient (Γ) is expressed with the normalized input impedance in equation (5).

$$Z_{i(1)} = \left(\frac{Z_1}{Z_2} \right)^2 \left(\frac{Z_3}{Z_4} \right)^2 \left(\frac{Z_5}{Z_6} \right)^2 Z_s = Z_{ip} \quad (3)$$

$$z = \frac{Z_{ip}}{Z_p} = \left(\frac{Z_1}{Z_2} \right) \left(\frac{Z_1}{Z_2} \right) \left(\frac{Z_3}{Z_4} \right) \left(\frac{Z_3}{Z_4} \right) \left(\frac{Z_5}{Z_6} \right) \left(\frac{Z_5}{Z_6} \right) \left(\frac{Z_s}{Z_6} \right) \quad (4)$$

$$\Gamma = \frac{z-1}{z+1} \quad (5)$$

where Z_p and Z_s are the characteristic impedances of the piezoelectric layer and silicon, respectively. And Z_1 to Z_6 are the characteristic impedances corresponding to the layers 1 to 6, respectively. The input impedances ($Z_{i(1)}-Z_{i(7)}$) are described in Fig. 2.

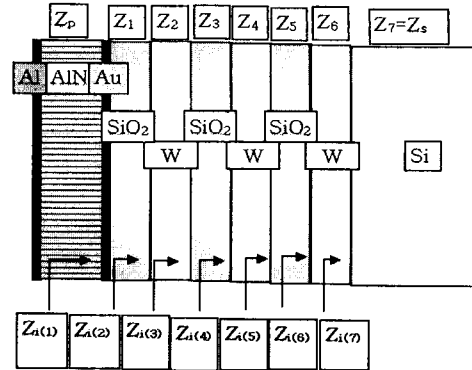


Fig. 2 Schematic impedance configuration.

The odd layers (SiO₂) have low impedance while the even layers (W) have high impedance. According to the equations (4) and (5), as the number of the stacked layers increases the normalized input impedance (z) of the acoustic multilayer reflector approaches zero and eventually the Γ will be -1. Therefore, the acoustic wave transmitting the piezoelectric layer fails to propagate into the substrate and it mostly reflects back at the reflector. Thus, the wave energy is confined within the piezoelectric layer. For the comparison, the Γ was calculated using equations (4) and (5) for various pairs of materials (Table 2). The AlN film deposited for the FBAR was observed to have small columnar grains with a strongly preferred orientation towards c axis, shown in Fig. 3. This is believed to result in superior resonance characteristics. In addition, S_{11} (return loss) and S_{21} (insertion loss) parameters were extracted from the two-port FBAR device (Fig. 1) with a resonance area of 150 x 150 μm^2 .

Table 2. Reflection coefficients of various multilayer pairs.

	SiO ₂ /W	SiO ₂ /AlN	Al/W	Al/AlN
1-layer	-0.511	-0.511	-0.423	-0.423
2-layer	-0.972	-0.781	-0.966	-0.733
3-layer	-0.985	-0.878	-0.977	-0.816
4-layer	-0.999	-0.952	-0.999	-0.9257
5-layer	-0.9997	-0.9745	-0.9993	-0.9506
6-layer	-0.99998	-0.9902	-0.99997	-0.9809

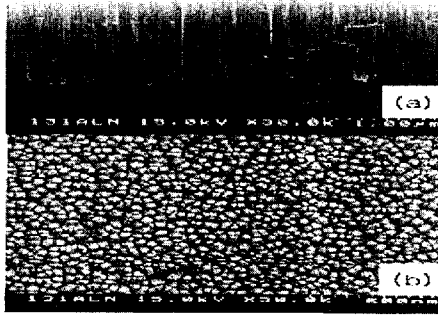


Fig. 3 SEM photographs of the deposited AlN films:

(a) cross-sectional view and (b) top view.

As a result, a good return loss of 37.19dB was obtained at center frequency of 1.983GHz along with an insertion loss of 6.13dB. The series resonance frequency(f_s) and parallel resonance frequency(f_p) were calculated as 1.976GHz and 2.005GHz, respectively. From these findings, the performance of the FBAR was evaluated using equations (6) and (7).

$$k_{eff}^2 = \frac{\frac{\pi}{2} \frac{f_s}{f_p}}{\tan\left(\frac{\pi}{2} \frac{f_s}{f_p}\right)} \approx \left(\frac{\pi}{2}\right)^2 \frac{f_p - f_s}{f_p} \quad (6)$$

$$Q_{s/p} = \frac{f_{s/p}}{2} \left| \frac{dZ_i}{df} \right|_{f_{s/p}} \quad (7)$$

K_{eff}^2 (the effective electromechanical coupling coefficient) is a measure of the relative frequency spacing between f_s and f_p and also determines the maximum bandwidth that can be achieved with a filter. $Q_{s/p}$ (the quality factor) is a measure of the resonator loss of a device at the series or parallel resonance frequency. Both K_{eff}^2 of 3.53% and $Q_{s/p}$ of 4300 were calculated.

IV. Conclusion

We present the fabrication and analysis results of a two-port FBAR device. The insertion loss(S_{21}) and return loss(S_{11}) were found 6.1 dB and 37.19 dB, respectively. In addition, a large quality factor(Q) of 4300 was also obtained. The FBAR technology appears to be very promising for 2 GHz RF bandpass filter applications.

References

- [1] M. Hikita, N. Shibagak, T. Akagi, and K. Sakiyama, "Design methodology and synthesis techniques for ladder-type SAW resonator coupled filters", IEEE Ultrasonics Symposium, pp. 15-24, 1993.
- [2] R. Ruby, and P. Merchant, "Micromachined thin film bulk acoustic resonators", Proc. Intl. Freq. Control Symposium, pp. 135-138, 1994.
- [3] J. S. Wang and K. M. Lakin, "Sputtered c-axis inclined ZnO films for shear wave resonators", Ultrasonic Symposium, pp. 480-483, 1982.
- [4] B. A. Auld., "Acoustic fields and waves in solids", Vol. I, Krieger Publishing Co., Florida, 2nd Ed., pp. 124-131, 1990.

저자소개



Giwan Yoon

1983 BS in Seoul National University
1985 MS in KAIST
1994 PhD in The University of Texas at Austin, USA
1985-1990: Associate Engineer, LG

Group, Semiconductor Research Center
1990-1994: RA, University of Texas at Austin, Microelectronics Center
1994-1997: Senior Engineer, Digital Equipment Corp. (Presently Intel), USA
1997-2000: Assistant Professor, Information and Communications University (ICU), Korea
2000-present : Associate Professor in ICU, Korea

※Area of interest: RF Device & Design, Smart Antenna & Smart Sensors, Bioelectronics



Munhyuk Yim

2002: BS in Material Engineering, Chungnam National University
2002-MS Course in ICU, Korea

※Area of interest: RF Device & Design, FBAR Filters, Ferroelectrics Devices

Dongkyu Chai

1999 BS in Electronic Engineering, Kyongbook University, Korea
2001-ICU, Korea

※Area of interest: RF Filter & Phase Shifter, Smart Sensors



Jongheon Kim

1985: BS in Kangwoon University
1990 MS in Ruhr University
1994 PhD in The University of Dortmund, Germany

※Area of interest: RF High Power Amplifier, Radio Spectrum Management, Linearization Techniques of Power Amplifier